Harmonic vibrations in two-dimensional graded elastic networks: Variety of normal modes and their transitions

J. J. Xiao,[1] K. Yakubo,[2] and K. W. Yu[1,3,*]
[1]*Department of Physics, The Chinese University of Hong Kong, Shatin, New Territories, Hong Kong, China*
[2]*Department of Applied Physics, Graduate School of Engineering, Hokkaido University, N13-W8, Sapporo 060-8628, Japan*
[3]*Institute of Theoretical Physics, The Chinese University of Hong Kong, Shatin, New Territories, Hong Kong, China*
(Received 2 March 2006; published 6 June 2006)

We study vibrational excitations in graded elastic networks modeled by coupled harmonic oscillators in a square lattice, in which the force constants or the vibrating masses can vary along one direction, i.e., the gradient direction. It turns out that the two-dimensional network under study can be reduced to a set of effective one-dimensional graded chains [Phys. Rev. B **73**, 054201 (2006)] with additional on-site potentials. We identify various kinds of vibrational normal modes in these networks with graded force-constant (mass), namely, unbound modes and two types of confined modes called soft (heavy) and hard (light) "gradons" which reside at the two opposite edges of the network in the gradient direction. The transitions from gradons to unbound modes occur at specific frequencies $\omega_{c1}(k_s)$ and $\omega_{c2}(k_s)$ for each corresponding wave number k_s in the transverse direction. While above the maximum of $\omega_{c2}(k_s)$, pure hard (light) gradons exist, there is severe mixing of nondegenerate phonons and gradons below this frequency, showing intriguing zigzag inverse participation ratio. It is very interesting to see such unusual excitation modes that have adjacent eigenvalues but possess quite different spatial extents. The results reduce to the previously obtained one-dimensional results for $k_s=0$. The method is quite general and applicable to three-dimensional elastic networks. We conclude with discussions on how these new gradon modes may affect the macroscopic properties of graded solids. Our results can also be applied to analogous systems with graded character.

DOI: 10.1103/PhysRevB.73.224201 PACS number(s): 63.20.Pw, 63.20.Dj, 63.22.+m

I. INTRODUCTION

Wave behavior in inhomogeneous or disordered media is an old subject,[1,2] but is still under great evolution upon new insights.[3–5] Wave propagation in these complex media is a large and interdisciplinary field of research with many unsolved problems that are scientifically challenging and technologically important.[6,7] Particular interest has been focused on the wave localization, either weak or strong. The concepts of weak and strong (i.e., Anderson) localization have originally been introduced in the study of electronic transport in metals where they are related to the metal-insulator transition.[1] With decreasing disorder, electron states change gradually from "strongly localized" to "weakly localized," and the energy levels become more correlated.

These concepts have also been applied to classical waves, e.g., ultrasonic waves, seismic waves, light waves, and microwaves, etc.[8] In particular, multiple-scattering conditions lead to interference effects that result in enhanced backscattering (i.e., weak localization) or strong localization of waves, whereas single impurity results in diffusive or localized waves.[7] These are, respectively, typical cases in randomly inhomogeneous medium[9] and in periodically modulated artificial structure with defect(s), e.g., spatial imperfections in a lattice.[10] Random media are ubiquitous, both in composites and materials in nature and, thus, have been extensively studied. On the contrary, impurities, in analogy to the donor or acceptor in semiconductors, are often carefully designed by including defect(s) into the otherwise periodic crystals.

Substantial insights have been gained regarding the aforementioned effects. However, much less is known about classical wave behaviors in gradually varied elastic or optical systems. In fact, there have been many studies on gradual variation of lattice anisotropy, i.e., gradual modification of the periodic crystals parameter, such as filling factor, lattice period, and/or intrinsic properties,[11] as well as on tapered optical elements[12] and chirped photonic crystals.[13] The effects of gradual variation of typical parameters on wave behavior (*graded effects*) have been noticed for quite a long time in terms of both elastic wave and light. Actually, in some cases gradient is much easier to be achieved than the precise control of impurities. Besides, there exist in nature abundant graded materials, such as biological cells[14] and liquid crystal droplets.[15] It has also been recognized that gradient can alter the wave dispersion relation and their density of modes. For example, Conwell first examined the electromagnetic wave guiding in graded-index layers that are formed by diffusion or liquid epitaxy.[16] Ye revisited the problem and applied the same spirit to interpret acoustic phenomena in ocean surface and bottom,[17] which are believed to possess gradient characters. As a matter of fact, graded-index fiber has attracted ever increasing interest over the past decades for communications; and a gradually changed interface is utilized to facilitate coupling light into and out of photonic crystals.[18]

Recently, one of the current authors, Yu and his coworkers, studied in detail graded composites[19] and naturally occurring materials with graded characters.[20] Very recently, we examined the elastic spectrum in a one-dimensional (1D) graded network and identified a different type of delocalization transition, namely, the phonon-gradon transition,[21] which is quite different from many well-established delocalization transitions. It also forms the basis for studying the

higher-dimensional graded systems. In this paper, we shall focus on elastic solids with a uniaxial gradient. These systems are modeled by graded harmonic spring-mass networks. We specifically study the vibrational spectrum and harmonic vibrational normal modes in the presence of a gradient in the force constants or masses and find out that some normal modes are confined at the edges of the network in the gradient direction, like the 1D gradons.[21] However, in contrast to the 1D case, we discover a reentrant localization-delocalization transition, that is, some counterintuitive confined modes at the low frequency regime, in addition to the high frequency gradons already discovered in the 1D case.[21] These modes reside at "soft"-springs ("heavy"-masses), while "hard"-springs ("light"-masses) confine high frequency modes which also appear in 1D graded elastic networks,[21] for a graded force constant model (graded masses model). It is quite interesting to see unusual excitation modes that have adjacent eigenvalues but possess quite different spatial extents. We further manage to explain the mechanism and offer explicit expressions of the reentrant transition frequencies. The broader significance of the present results and their relevance to general physical phenomena, however, remain to be revealed.

In what follows, we first briefly describe, in Sec. II, the graded elastic network model, and establish the formalism for studying the eigenmodes. In Sec. III, we present our results mainly in the case of graded force constant. Finally, conclusions and some discussions on our results are given.

II. GRADED ELASTIC NETWORK MODEL

The elastic problem in high dimensions can be modeled by a simple square (cubic) lattice of size N^2 (N^3) with lattice constant $a=1$, in which masses at nearest-neighboring sites r and q are connected by a spring with force constant K_{rq} which is assumed to be a scalar force constant. The Hamiltonian of the harmonic lattice is of the form

$$H = \sum_{q=1}^{N^d} \frac{P_q^2}{2m_q} + \sum_{q=1}^{N^d} \sum_{r} \frac{1}{2} K_{rq}(u_r - u_q)^2, \tag{1}$$

where $\{u_q, P_q, m_q\}$ denote the position, i.e., the scalar displacement about equilibrium position, momentum, and mass of particle at the site q. In Eq. (1) d denotes the spatial dimension of the system, e.g., $d=2$ indicates a square lattice in two dimensions (2D), which we shall exemplify in this work. In this case q and r label the sites in the square lattice as $q=(N-1)i+j$ for $i=1,2,\ldots,N$ and $j=1,2,\ldots,N$. The sum on r runs over the nearest-neighboring sites of q with $r<q$. In this regard, each site q is assigned to d bonds with force constant K_{rq} that are connected to it in a directional way. Thus we get the following equation of motion:

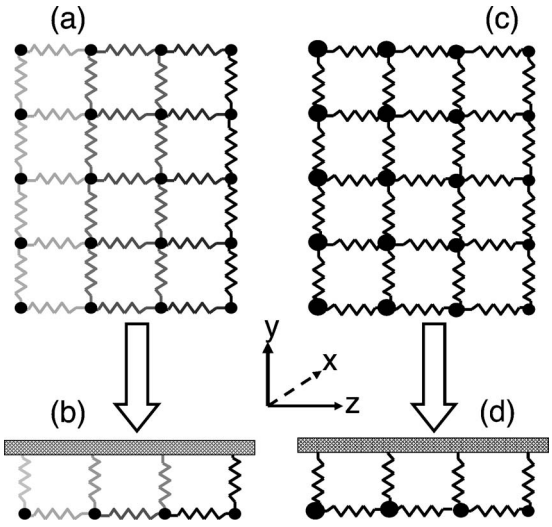

FIG. 1. (a) Schematic diagram of a two-dimensional graded force constant system. (b) The reduced one-dimensional graded system with additional springs (springs connected to the ceiling) corresponding to (a). (c) Schematic diagram of a two-dimensional graded mass system. (d) The effective one-dimensional graded system with additional springs.

$$m_q \frac{d^2 u_q(t)}{dt^2} = \sum_{r} K_{rq}[u_r(t) - u_q(t)] \tag{2}$$

for all spatial components of the particle displacement u_q. We further assume a gradient in the force constant or mass in one spatial direction, e.g., along z axis, which is referred to the gradient direction or the longitudinal direction. We also enforce periodic boundary conditions in the directions perpendicular to the gradient direction $\hat{z}$. That is denoted as the transverse direction, e.g., x and/or y axis as shown in Fig. 1. Then by decomposing the amplitude u_q with the eigenvectors $\boldsymbol{e}(\lambda)$ of the mode λ as $u_q=\Sigma_\lambda Q_\lambda(t)\boldsymbol{e}(\lambda)$, where $Q_\lambda(t)$ is a time-dependent expansion coefficient which behaves as $Q_\lambda(t)\sim\exp(-\mathbf{i}\omega_\lambda t)$, Eq. (2) is partially decoupled and reduced to an effective 1D eigenproblem of coupled harmonic oscillators

$$m_i\omega^2 e_i = \left(K_{i-1}^{\mathrm{L}} + K_i^{\mathrm{L}} + 2K_i^{\mathrm{T}} \sum_{\alpha=1}^{d-1} [1 - \cos k_s^{(\alpha)}] \right) e_i - K_{i-1}^{\mathrm{L}} e_{i-1} - K_i^{\mathrm{L}} e_{i+1}, \tag{3}$$

where $i=1,2,\ldots,N$ label the layers along the gradient direction $\hat{z}$ and m_i denotes the point mass at sites included in the ith layer. Since the gradient is uniaxial, the eigenvector $\boldsymbol{e}(\lambda)$ can be written in the form of $e_q=e_i\exp[\mathbf{i}\Sigma_\alpha k_s^{(\alpha)} x_\alpha(l)]$, where l labels the site in the ith layer, $k_s^{(\alpha)}$ with $\alpha=1,\ldots,d-1$ represents the transverse wave number, and $x_\alpha(l)$ denotes the α component

of the position vector of the site l in the transverse $(d-1)$ dimensional space. Because periodic boundary conditions must be satisfied in the transverse direction, in Eq. (3) we must let $k_s^{(\alpha)}=2\pi s/N$, where $s=0,1,\ldots,N-1$ being an integer. The graded force constants are assumed to be locally isotropic and represented by the longitudinal K_i^{L} and the transverse K_i^{T}, respectively. For a linear gradient model,

$$K_i^{\mathrm{L}} = K_0 + \frac{C_K(i-1)}{N-1} \quad (i=1,2,\ldots,N-1), \tag{4a}$$

$$K_i^{\mathrm{T}} = \frac{K_i^{\mathrm{L}} + K_{i-1}^{\mathrm{L}}}{2} \quad (i=2,\ldots,N-1), \tag{4b}$$

while $K_0^{\mathrm{L}}=K_N^{\mathrm{L}}=0$, $K_1^{\mathrm{T}}=K_0-C_K/2(N-1)$, and $K_N^{\mathrm{T}}=K_0+C_K(N-3/2)/(N-1)$. In this locally isotropic force constant model, Eqs. (4a) and (4b), however, characterize an anisotropic system with a linear gradient in the force constant along the uniaxial axis (e.g., z axis) in one of the orthogonal directions of the square lattice, i.e., with a base force constant K_0 and a gradient coefficient C_K in the force constant. Specifically, in 2D case we can omit the superscript (α) in $k_s^{(\alpha)}$ because $\alpha=1$ in this case, therefore we will use k_s to denote the transverse wave number in the 2D case hereafter.

In conclusion, we have simplified a size-N^d problem [Eq. (2)] to size-N one-dimensional problems as depicted by Eq. (3) with N^{d-1} different values of $k_s^{(\alpha)}$, which is equivalent to a 1D graded chain[21] with additional on-site potentials $V_i=2K_i^{\mathrm{T}}\Sigma_{\alpha=1}^{d-1}[1-\cos k_s^{(\alpha)}]$. In the graded mass model, we alternatively have $m_i=m_0-C_m i/N$ where C_m is the coefficient of the graded mass and m_0 is the base mass. In this case, we keep the force constant K_i^{L} and K_i^{T} to be uniform across the whole lattice. Setting $C_K=0$ (or $C_m=0$) recovers the system homogeneous. Pictorial illustrations of the aforementioned reducing processes are shown in Fig. 1.

III. RESULTS

Without loss of generality, in this section we will mainly discuss the results of square lattices with graded *force constant*. The analyses are applicable to the graded mass case and similar results are found. Following the method as outlined in the 1D case,[21] we diagonalize the eigenvalue problem of coupled harmonic oscillators with graded force constant as described by Eqs. (3) and (4). Open boundary conditions, i.e., $K_0^{\mathrm{L}}=0$ and $K_N^{\mathrm{L}}=0$, are used in the gradient direction (e.g., z axis). Dispersion relations always have fundamental interest, which also reflect the density of normal modes. But in the graded elastic network, the wave number is not conserved in the gradient direction because of the lack of translational symmetry in this direction. This does not allow us to consider the dispersion relation for our model. Nevertheless, relations between the eigenfrequency ω_λ and the mode index λ in ascending order for every fixed transverse wave number k_s, which can be regarded as a pseudo-dispersion relations, help us to interpret vibrational modes in the graded system. In what follows, we may use a set of indices to denote the normal mode λ, i.e., $\lambda=(k_s,n_{\mathrm{L}},\omega)$,

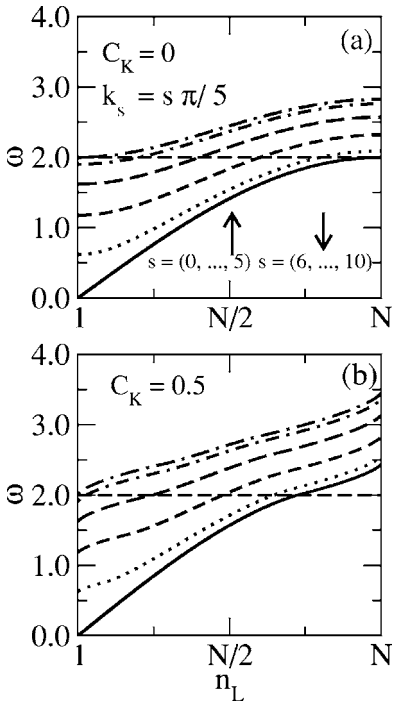

FIG. 2. Pseudodispersion relations between n_{L} and ω for various k_s for (a) homogenous 2D network ($C_K=0$) and (b) graded network ($C_K=0.5$). Results in (a) can also be regarded as the usual dispersion relations.

where n_{L} and ω label the (longitudinal) mode index for a specific transverse wave number k_s and the mode frequency, respectively.

The pseudodispersion relations between n_{L} and ω are shown in Figs. 2(a) and 2(b) for the graded coefficient $C_K=0$ (i.e., homogeneous network) and $C_K=0.5$, respectively, with various $k_s=s\pi/5$, where $s=0,1,\ldots,9,10$. The results are obtained with $m_i=m_0=1$ (i.e., $C_m=0$), $K_0=1$, and $N=1000$. Figure 2(a) is for the homogenous network with $K_i^{\mathrm{T}}=K_i^{\mathrm{L}}=1$ and $m_i=1$, which can be regarded as the usual dispersion relations. From these (pseudo) dispersion relations, it is clear that the modes $\lambda=(k_s,n_{\mathrm{L}},\omega)$ are doubly degenerated for k_s. For example, the curves representing pseudodispersion relations between n_{L} and ω for $s=10,9,8,7,6$ overlap those for $s=0,1,2,3,4$, respectively (see Fig. 2).

Note that in Fig. 2(b) when $k_s=0$ (solid curve), one recovers a pure 1D graded chain of coupled harmonic oscillators, which we have elucidated in great detail.[21] With vanishing k_s, in comparison to the homogeneous network [Fig. 2(a)], the pseudo-dispersion relations are altered significantly only for $\omega>\omega_c=2.0$. As we already discussed,[21] the modes appearing at $\omega>2.0$ are identified to be gradons and are confined at "hard" springs (or at light masses in the graded mass model). However, a significant difference appears for nonvanishing k_s $(s\neq 0)$, for which we observe two oscillations in the pseudodispersion relation curves. The oscillations indicate phase transitions, which do not appear at the zone-folding band edge as in the homogeneous case [see the dashed or dotted curves in Figs. 2(a) and 2(b), respectively]. As a matter of fact, these figures are projections of those shown in Fig. 3, in which the eigenfrequencies ω are shown

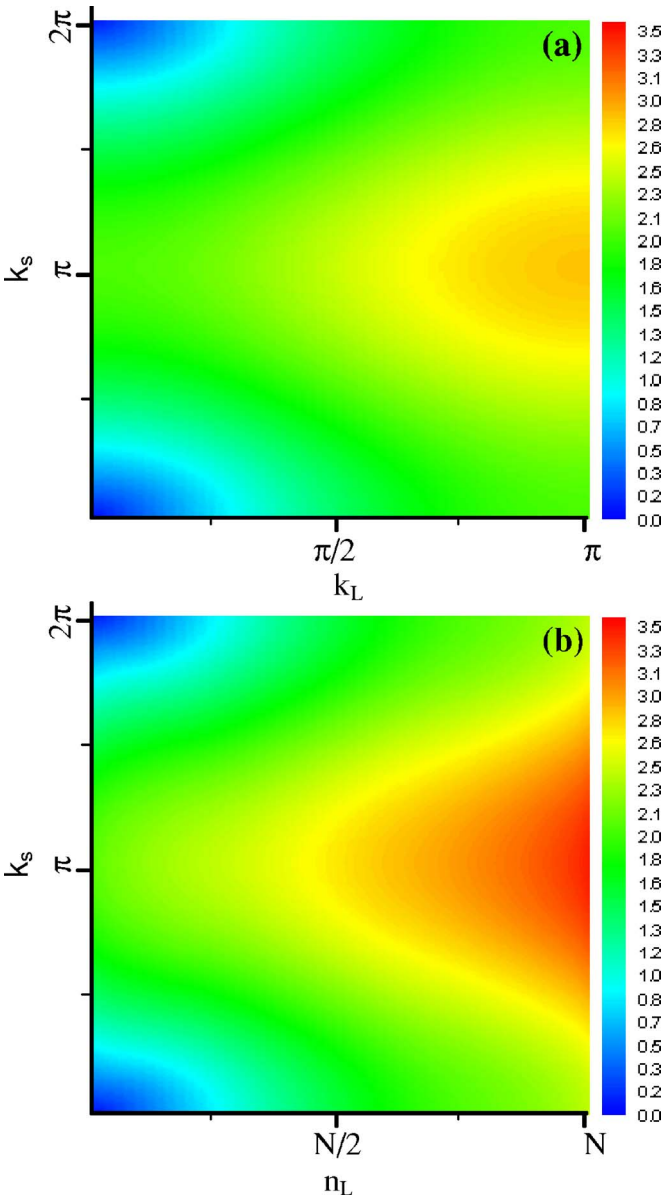

FIG. 3. (Color online) Contour plot of eigenfrequency ω for the transverse wave number k_s and the longitudinal eigenmode index n_L for (a) homogeneous 2D network with $C_K=0$ and (b) graded network with $C_K=0.5$.

as a contour plot of the transverse wave number k_s and the (reduced) longitudinal mode index n_L. Figure 3(a) is for the homogeneous square network and we replace its horizontal axis n_L by the longitudinal wave number k_L, whereas Fig. 3(b) is for the graded square network, on the same scale of frequency as in Fig. 3(a).We can clearly see that the presence of gradient significantly alters the isofrequencies, particularly near $k_s=\pi$, i.e., at the band edge or along the lines in the irreducible Brillouin zone joining the high symmetry points along the transverse direction.

To examine precisely the expected transitions from Fig. 2(b), we show the density of states (DOS) in Fig. 4. In the upper panels [Figs. 4(a) and 4(b)] of this figure, we actually plot the partial density of states (PDOS)

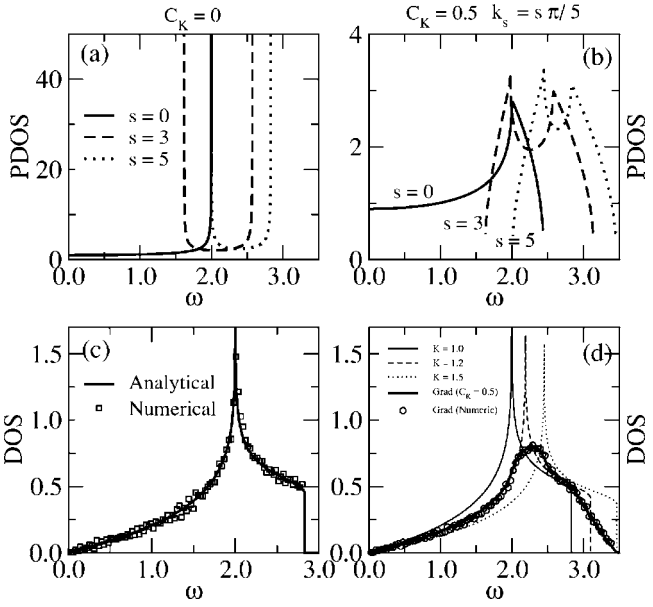

FIG. 4. Partial density of states for (a) homogeneous 2D network ($C_K=0$) and (b) graded network ($C_K=0.5$). The total densities of states obtained numerically (symbols) and analytically (curves) are also presented for (c) homogeneous and (d) graded cases.

$$D(\omega,k_s)=\frac{1}{N}\sum_{\lambda\in S(k_s)}\delta(\omega-\omega_\lambda) \tag{5}$$

as a function of frequency for $k_s=s\pi/5$ with $s=0$, 3, and 5. Here, $S(k_s)$ represents the set of modes having the transverse wave number k_s. The PDOS shown here can be regarded as the inverse of derivative of the curves shown in Fig. 2. It is clearly seen in Fig. 4(b) that there are two peaks in the PDOS for nonvanishing k_s ($s\neq 0$): One peak appears in the low-frequency $[\omega_{c1}(k_s)]$ region and the other at relatively higher frequencies $[\omega_{c2}(k_s)]$. As k_s approaches π, both $\omega_{c1}(k_s)$ and $\omega_{c2}(k_s)$ increase monotonously from 0 to 2.449 and from 2.0 to $\omega_{\max}$, respectively, where $\omega_{\max}\equiv 2\sqrt{2(K_0+C_K)/m_0}\approx 3.464$ is the maximum eigenfrequency of the harmonic vibrational modes supported by the graded square lattice. Additionally, the (usual) total vibrational density of states

$$D(\omega)=\frac{1}{N^d}\sum_{s=1}^{N^{d-1}}\sum_{\lambda\in S(k_s)}\delta(\omega-\omega_\lambda) \tag{6}$$

are shown in Figs. 4(c) and 4(d) for the homogeneous case (□) and for the graded case (○), respectively. Note that in obtaining the histogram of DOS we have used frequency bin $\Delta\omega=0.0283$ and 0.0342 in Figs. 4(c) and 4(d), respectively. The sharp peak (Van Hove singularity) of the DOS for the homogeneous network is somehow rounded and even disappears in the case of graded network. This is also reflected by the contour plot in Fig. 3. In Fig. 3(b) the green region representing $\omega\approx 2.0$ diminishes, while the orange region representing $\omega\approx 2.8$ expands, as compared to Fig. 3(a). In fact, the DOS of an infinite graded elastic network can be expressed as an average of the DOS's of homogeneous networks over a range of force constants. The arguments are as

follows. Let us slice the infinite graded network along the gradient direction into many subnetworks each still being infinite in size (i.e., no boundary effects). For each subnetwork, the gradient is infinitesimal so that it can be regarded as a homogeneous network. Thus, the DOS of a homogeneous network can be used to describe each subnetwork. In this way, the DOS of the infinite graded network can be expressed as an average of the DOS of the subnetwork over a range of force constants. Specifically, for a 2D square lattice of homogeneous media with point mass M and force constant K, the DOS can be expressed as[22]

$$g(\omega,M,K) = \begin{cases} \dfrac{4}{\pi^2\sqrt{\omega_L^2-\omega^2}}F(\nu), & \omega^2(\omega_L^2-\omega^2) > 16\beta^2, \\ \dfrac{\omega}{\pi^2\beta}F\left(\dfrac{1}{\nu}\right), & 0 < \omega^2(\omega_L^2-\omega^2) < 16\beta^2, \\ 0, & \text{otherwise}, \end{cases} \tag{7}$$

where $\beta^{1/2}=\sqrt{K/M}$ is the intrinsic frequency, $\omega_L^2=8\beta$ denotes the maximum frequency, $F(x)$ is the complete elliptic integral of the first kind, and

$$\nu = \frac{4\beta}{\omega\sqrt{\omega_L^2-\omega^2}}. \tag{8}$$

Consequently, the DOS of the graded system we studied with $M=m_0=1$ [see Eqs. (3) and (4)] can be obtained by the following integration:

$$g_G(\omega) = \frac{1}{C_K}\int_{K_0}^{K_0+C_K} g(\omega,1,K)dK. \tag{9}$$

The results for infinite size of the homogeneous case from Eq. (7) and for the graded case from Eq. (9) are also shown by thick solid curves in Figs. 4(c) and 4(d), respectively. Furthermore, a series of DOS of the homogeneous case with $K=K_0=1.0$ (thin solid curve), $K=1.2$ (thin dashed curve), and $K=K_0+C_K=1.5$ (thin dotted curve) are also plotted in Fig. 4(d). It is clearly seen that the results from these closed forms (curves) agree very well with the numerical data (symbols). It is further noticed that the low frequency part of the DOS for the graded network with $C_K=0.5$ almost coincides with that for the homogeneous network with $K=1.2$ [Fig. 4(d)]. This is related to the effective medium theory. The force constant of an effective homogeneous media for $C_K=0.5$ is $K_{\text{eff}}=\{\int_0^1 dx[1/(1+0.5x)]\}^{-1}\approx 1.233$. In this regard, at low frequencies, the graded network can be regarded as an effective homogeneous medium with $K=K_{\text{eff}}$. The DOS of a graded mass network of infinite size can be obtained in a similar way.

In view of the clear transition features indicated in the PDOS, we expect that the modes fall in $0<\omega<\omega_{c1}(k_s)$, $\omega_{c1}(k_s)<\omega<\omega_{c2}(k_s)$, and $\omega>\omega_{c2}(k_s)$ are qualitatively different from each other. Indeed, we see a reentrant localization-delocalization transition in the longitudinal mode pattern, i.e., we plot in Fig. 5(b) the eigenfunction of

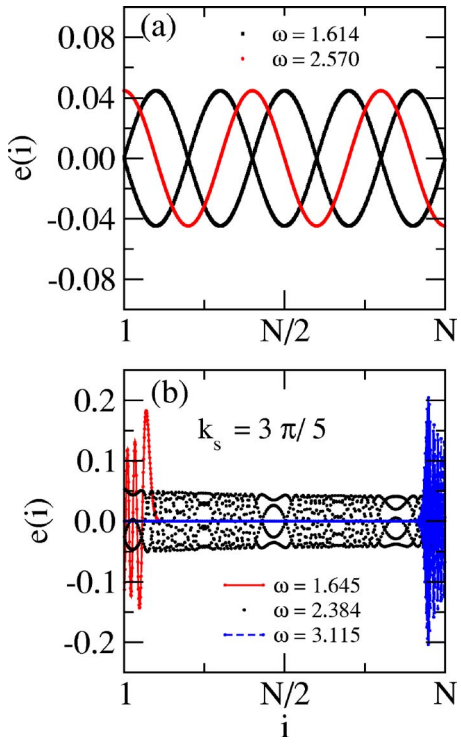

FIG. 5. (Color online) Mode pattern in (a) homogeneous lattice ($C_K=0$) for $\omega=1.614$ and $\omega=2.570$ and (b) graded lattice ($C_K=0.5$) for three typical frequencies $\omega=1.645$ [$0<\omega<\omega_{c1}(3\pi/5)$], $\omega=2.384$ [$\omega_{c1}(3\pi/5)<\omega<\omega_{c2}(3\pi/5)$], and $\omega=3.115$ [$\omega>\omega_{c2}(3\pi/5)$].

$\boldsymbol{e}(\lambda)=\{e_i\}$ as a function of the layer index i for three typical frequencies of $\omega=1.645$, $\omega=2.384$, and $\omega=3.115$, respectively. In particular, the mode of high frequency $\omega=3.115$ is confined at hard-springs (i.e., those with larger K^L), like a gradon in 1D graded chain.[21] The mode of intermediate frequency $\omega=2.384$ is extended across the whole network. However, the low frequency mode $\omega=1.645$ is shown to be localized as well, but rather on the soft-spring side. These are substantially different from results in 1D.[21] In Fig. 5(b), $k_s=3\pi/5$ is used as an example, but we have examined many modes for other k_s and found similar results except for $k_s=0$, for which the low frequency localization disappears, i.e., $\omega_{c1}(k_s)\to 0$ when $k_s\to 0$. A detailed discussion for $k_s=0$ corresponding to the 1D case has been carried out.[21] Note that for homogeneous square network, there is no such reentrant transition, as seen in Fig. 5(a), where all modes are extended for any frequency, either high, intermediate, or low.

Therefore, we have identified two transitions which are in accordance to the emergence of two kinds of longitudinally confined modes. More precisely, for certain k_s, higher energy excitations are bounded at hard-springs and those with lower energies are bounded in the soft-spring side. We name these modes "hard gradons" and "soft gradons," respectively. We numerically plot the transition frequencies $\omega_{c1}(k_s)$ and $\omega_{c2}(k_s)$ versus k_s in Fig. 6(b) by filled squares and triangles, respectively. Open triangles and circles represent the maximum and minimum frequencies of modes, namely the upper and lower cut-off frequencies of the PDOS as shown in Fig. 4(b). For comparison, results for a homogeneous square net-

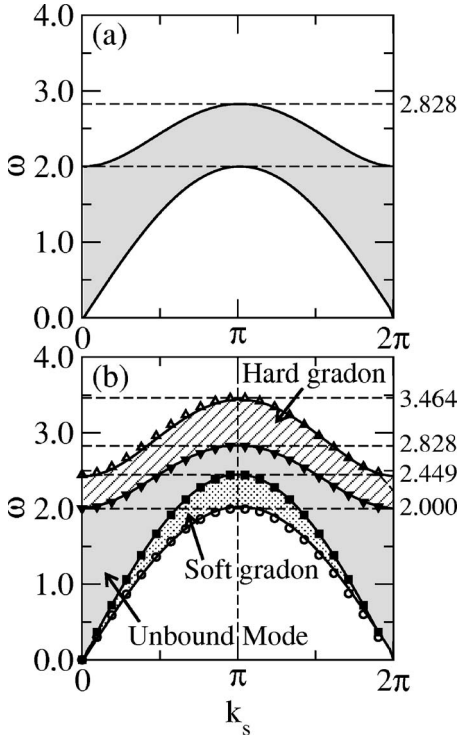

FIG. 6. Phase diagram in the k_s-ω space for (a) homogenous network (C_k=0) and (b) graded network (C_K=0.5). Results in (a) can be regarded as the usual dispersion relation. Frequencies of soft and hard gradons in (b) are in agreement with analytical predictions (solid lines).

work with $m_0=1$ and $K_0=1$ are plotted in Fig. 6(a). In this case, all modes are extended as well known.

Figure 6(b) clearly demonstrates partitions of the normal vibrational modes in the 2D graded lattice and can be regarded as a phase diagram. That is, the vibrational normal modes of the square lattice with uniaxially graded force constants have been categorized into three types: Soft gradons (S), unbound modes (U), and hard gradons (H). The confinement of the soft gradons is quite distinguished because it is in the lower frequency regime. The confinement mechanism of the soft gradons can be explained as a consequence that a low frequency vibrational mode can be excited only in a spatial region in which additional springs [e.g., springs connected to the ceiling in Fig. 1(b)] are soft enough to excite such a low frequency mode, which is expected, for the constant $m_i(=m_0)$ case, to happen at $\omega_{\mathrm{low}}^{(\mathrm{soft})}(k_s)<\omega<\omega_{\mathrm{up}}^{(\mathrm{soft})}(k_s)$, where

$$\omega_{\mathrm{low}}^{(\mathrm{soft})}(k_s)=\sqrt{\frac{K_{\mathrm{min}}^{*}}{m_0}}, \tag{10a}$$

$$\omega_{\mathrm{up}}^{(\mathrm{soft})}(k_s)=\sqrt{\frac{K_{\mathrm{max}}^{*}}{m_0}}. \tag{10b}$$

Here, K_{min}^{*} and K_{max}^{*} are the minimum and maximum force constants of the additional springs, which are generally given, from Eqs. (3) and (4), by

$$K_{\mathrm{min}}^{*}=2K_0\sum_{\alpha=1}^{d-1}[1-\cos k_s^{(\alpha)}], \tag{11a}$$

$$K_{\mathrm{max}}^{*}=2(K_0+C_K)\sum_{\alpha=1}^{d-1}[1-\cos k_s^{(\alpha)}] \tag{11b}$$

for an infinite graded force constant system. Therefore, the soft gradons in two dimensions are excited in the frequency region of

$$\sqrt{\frac{2K_0(1-\cos k_s)}{m_0}}<\omega<\sqrt{\frac{2(K_0+C_K)(1-\cos k_s)}{m_0}}. \tag{12}$$

It is reasonable that the frequencies $\omega_{\mathrm{low}}^{(\mathrm{soft})}(k_s)$ and $\omega_{\mathrm{up}}^{(\mathrm{soft})}(k_s)$ give the lowest frequency of modes with k_s and $\omega_{c1}(k_s)$, respectively. In fact, the lower two solid lines in Fig. 6(b) representing $\omega_{\mathrm{low}}^{(\mathrm{soft})}(k_s)$ and $\omega_{\mathrm{up}}^{(\mathrm{soft})}(k_s)$ agree quite well with our numerical results (symbols ○ and ■). We further note that the lower and upper bounds of hard gradon frequencies are given by

$$\omega_{\mathrm{low}}^{(\mathrm{hard})}(k_s)=\sqrt{\frac{4K_{\mathrm{min}}^{\mathrm{L}}+K_{\mathrm{min}}^{*}}{m_0}}, \tag{13a}$$

$$\omega_{\mathrm{up}}^{(\mathrm{hard})}(k_s)=\sqrt{\frac{4K_{\mathrm{max}}^{\mathrm{L}}+K_{\mathrm{max}}^{*}}{m_0}}, \tag{13b}$$

where $K_{\mathrm{min}}^{\mathrm{L}}$ and $K_{\mathrm{max}}^{\mathrm{L}}$ are the minimum and maximum values of K_i^{L}, respectively. That is, from Eq. (4a), $K_{\mathrm{min}}^{\mathrm{L}}=K_0$ and $K_{\mathrm{max}}^{\mathrm{L}}=K_0+C_K$. This is because high frequency vibrational modes can be excited only in a spatial region in which the local stiffness is high enough to excite such high frequency modes. In 2D, using Eqs. (13), we get $\omega_{\mathrm{low}}^{(\mathrm{hard})}(k_s)=\sqrt{2K_0(3-\cos k_s)/m_0}$ and $\omega_{\mathrm{up}}^{(\mathrm{hard})}(k_s)=\sqrt{2(K_0+C_K)(3-\cos k_s)/m_0}$. These two characteristic frequencies $\omega_{\mathrm{low}}^{(\mathrm{hard})}(k_s)$ and $\omega_{\mathrm{up}}^{(\mathrm{hard})}(k_s)$ can be regarded as $\omega_{c2}(k_s)$ and the maximum frequency of modes with k_s, respectively. The k_s dependences of $\omega_{\mathrm{low}}^{(\mathrm{hard})}(k_s)$ and $\omega_{\mathrm{up}}^{(\mathrm{hard})}(k_s)$ are shown by the upper two solid lines in Fig. 6(b). Again, the numerical and analytical results of the frequency bounds for hard gradons are in excellent agreements. It should be noted that $\omega_{\mathrm{low}}^{(\mathrm{soft})}(0)=\omega_{\mathrm{up}}^{(\mathrm{soft})}(0)=0$, $\omega_{\mathrm{low}}^{(\mathrm{hard})}(0)=2$ and $\omega_{\mathrm{up}}^{(\mathrm{hard})}(0)=2.449$ exactly reproduce (hard) gradons in a 1D graded system.[21]

The phase diagram of Fig. 6(b) is of great interest from the perspective of excitation energy. There exist four characteristic regions separated by the four horizontal dashed lines.

(i) In the lowest frequency region,

$$0<\omega<\omega_{\mathrm{low}}^{(\mathrm{soft})}(\pi)\quad(\text{namely, } 0<\omega<\sqrt{4K_0/m_0}=2), \tag{14}$$

the spectra contain soft gradons and unbound modes ($S+U$).

(ii) The region of

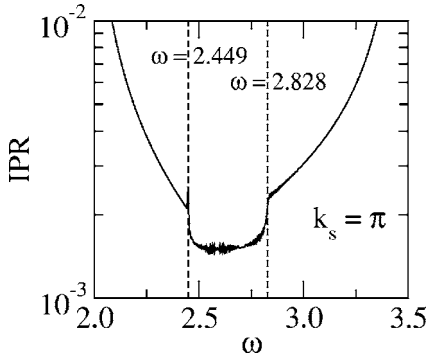

FIG. 7. Inverse participation ratio (IPR) for modes with $k_s=\pi$ as a function of frequency ω.

$$\omega_{\mathrm{low}}^{(\mathrm{soft})}(\pi) < \omega < \omega_{\mathrm{up}}^{(\mathrm{soft})}(\pi) \quad (\text{namely, } 2 < \omega < \sqrt{4(K_0 + C_K)/m_0} \approx 2.449) \tag{15}$$

contains soft gradons, unbound modes, and hard gradons $(S+U+H)$.

(iii) The region of

$$\omega_{\mathrm{up}}^{(\mathrm{soft})}(\pi) < \omega < \omega_{\mathrm{low}}^{(\mathrm{hard})}(\pi) \quad (\text{namely, } 2.449 < \omega < \sqrt{8K_0/m_0} \approx 2.828) \tag{16}$$

has hard gradons and unbound modes $(H+U)$.

(iv) The highest frequency region,

$$\omega_{\mathrm{low}}^{(\mathrm{hard})}(\pi) < \omega < \omega_{\mathrm{up}}^{(\mathrm{hard})}(\pi) \quad (\text{namely, } 2.828 < \omega < \sqrt{(K_0 + C_K)/m_0} \approx 3.464) \tag{17}$$

contains only hard gradons (H).

It is quite interesting that such a simple system has so wide varieties. The reentrant transitions for fixed $k_s=\pi$ from gradons to extended modes are clearly illustrated by the inverse participation ratio[21,23,24] (IPR) as shown in Fig. 7. The IPR is of the order of $1/N$ if the mode is extended, while becomes larger when the mode is confined within a small spatial region. Figure 7 definitely proves the existence of the reentrant transition between gradons and unconfined modes (phonons).

It is also remarkable that modes with adjacent eigenvalues possess quite different spatial extents in the regions (i)–(iii). This situation is illustrated by Fig. 8 in which the IPRs for the effective 1D chain are plotted versus frequency ω. In Fig. 8 a zigzag IPR curve indicates a very complicated frequency dependence of spatial extents of modes. In the frequency regions (i)–(iii), modes alternate localized and extended states depending on k_s. The localization length of soft gradons decreases with the frequency in region (i), while it has a maximum value (i.e., minimum in the IPR) in region (ii). In region (iii), the localization length of hard gradons again decreases with ω. In contrast to regions (i)–(iii), there are no unbound modes in region (iv), which can be seen from larger values of the smallest IPR in this region. These behaviors of the IPR are consistent with the phase diagram Fig. 6(b).

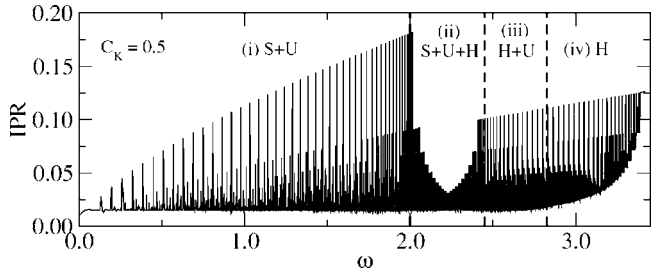

FIG. 8. IPR vs frequency ω for all the modes in the graded square network.

Due to the duality between force constant and mass, the graded mass model is essentially the same with the graded force constant model we discussed. Similarly, in the graded mass case [Figs. 1(c) and 1(d)], we substantially find the same confined modes, which reside in "light" masses at higher frequencies and in "heavy" masses at lower frequencies, and are thus called "light gradons" and "heavy gradons," respectively. In this case, $\omega_{\mathrm{low}}^{(\mathrm{heavy})}(k_s)=\sqrt{K^*/m_{\max}}$ and $\omega_{\mathrm{up}}^{(\mathrm{heavy})}(k_s)=\sqrt{K^*/m_{\min}}$ represent the bounds of heavy gradon frequencies, where $K^*=2K_0[1-\cos k_s^{(\alpha)}]$ denotes the force constant mediated by the additional on-site potential and $m_{\max}$, $m_{\min}$ are, respectively, the maximum and the minimum masses in the graded mass network. Similarly, the bounds of light gradons $\omega_{\mathrm{low}}^{(\mathrm{light})}(k_s)$ and $\omega_{\mathrm{up}}^{(\mathrm{light})}(k_s)$ are given by substituting with $K^*=2K_0[3-\cos k_s^{(\alpha)}]$ in the above expressions for heavy gradons. In the same way as adopted in Fig. 6(b), a phase diagram for heavy gradons, unbound modes, and light gradons can be obtained.

IV. DISCUSSION AND CONCLUSION

In summary, we have identified various kinds of vibrational normal modes in 2D graded elastic networks, namely, unbound modes and confined modes called soft (heavy) and hard (light) "gradons" which reside at the two opposite edges of the network in the gradient direction. The dependences of the lower and upper frequency bounds on the transverse wave number k_s have been analytically determined for an infinite graded system. For a fixed k_s, we have discovered a reentrant transition due to the competition between the transverse momentum and the longitudinally effective confinement. It is obvious that the three-dimensional results of a graded solid are basically the same, in view of their similarity of the reduced effective 1D problem as described by Eq. (3), i.e., the presence of additional dimension(s) only introduces additional on-site potentials to the 1D graded elastic chain.[21] Although we mainly present the results in 2D square lattices with orthogonal gradient, soft (heavy) and hard (light) gradons would exist also in square lattices with diagonal gradient, as well as in triangular lattices with a nontrivial gradient. In this regard, the method we demonstrated for the reduction of inhomogeneous problem in higher dimensions to equivalent 1D problems is applicable to a wide spectrum of systems. For example, by virtue of the analogy of the vibrational problem with many other problems, such as electromagnetic wave propagation[25,26] in which the index

of refraction plays the same role as the mass, one would expect similar reentrant transitions from soft (heavy) and hard (light) gradons to extended modes. In particular, in quantum systems with graded characters,[27] analogies between the classical and quantum problems indeed lead to many cross fertilizations since solutions obtained in one field can be carried over to the other.

The model we considered here may have relevance to carbon nanotubes which are made by wrapping graphitic sheets into cylindrical structures. However, they have no simple square or rectangular lattices. A gradient in the azimuthal direction is possible with various ambients of the nanotube, which will alter the dispersion and the DOS of vibrational modes. This may lead to interesting electron-gradon interactions in this system. The electrostatic interactions effectively increase the elastic moduli near the surface region of a nanotube, leading to a suppression of the strain.[28] Since the effective force constant is related to the charge density in piezoelectric materials, the force constants are expected to vary as well. The piezoelectric property of nanotubes thus may give a possibility to observe gradons by electrical measurements. In addition, some changes in the heat capacity of graded elastic solids would be visible around $T_c = \hbar\omega_{c1}(\pi)/K_B$ and $\hbar\omega_{c2}(\pi)/K_B$ (K_B the Boltzman constant) with respect to that of a homogeneous media, by simply utilizing the DOS shown in Figs. 4(c) and 4(d). The remarkable change in the DOS of graded networks may be detected by Mössbauer spectroscopy because its effect in the recoiless fraction,[29] or by other sensitive spectroscopies such as nuclear magnetic resonance spectroscopy due to gradons possible effects on the nuclear spin-lattice relaxation rate.[30] Using the conventional neutron scattering method on the graded system will also be informative.

It would be interesting to study the transmission coefficient/transmission probability,[31] energy flow,[32] and heat conduction[33] versus the graded coefficient C_K or C_m. Our current results are relevant to a variety of problems like vibrational DOS of nanoscopic grains[34] and transportation through nanoscale devices that possess graded characters. The effects of gradient on the wave transmission coefficient are expected to be significant. For example, the high-transmission extended excitations might become squeezed and more confined modes appear with low transmission at the pure band of hard gradons [e.g., region (iv) by Eq. (17)]. Specifically, from the phase diagram Fig. 6(b) we expect very low transmission in the frequency range of $\omega > 2.0$ because a majority of modes are confined beyond the frequency of 2.0 in the case we analyzed. Simulations of the propagation of a wave packet in graded systems will reveal these behaviors.

Sound waves in graded materials also affect how light moves through it, because the compression effect of the sound changes the refractive index from place to place, which is the acousto-optic effect. It can be measured by sending a sound wave into the structure and measuring what it does to a beam of light reflected by it, optimizing the interaction between sound and light, for example, in selectively filled porous silicon. In this context, the frequency-dependent reentrant transition behaviors in graded materials will definitely lead to flexibly controllable acousto-optic effects. Finally, in terms of exciting the eigenmodes in the graded system, it should be remarked that an excitation launched outside the system must have a plane wave component with wave number $k > k_s$. In some cases, we may be able to construct structures having a complete band gap for acoustic waves[35] or light with the help of hard or light gradons.

ACKNOWLEDGMENTS

The authors would like to acknowledge useful discussions with T. Nakayama. This work was supported in part by RGC Earmarked Grant of the Hong Kong SAR Government (K.W.Y.), and in part by a Grant-in-Aid for Scientific Research from Japan Society for the Promotion of Science (Grant No. 16360044).

*Electronic address: kwyu@phy.cuhk.edu.hk

[1] P. W. Anderson, Phys. Rev. **109**, 1492 (1958).
[2] *Scattering and Localization of Classical Waves in Random Media*, edited by P. Sheng (World Scientific, Singapore, 1990).
[3] M. A. Kaliteevski, J. M. Martinez, D. Cassagne, and J. P. Albert, Phys. Rev. B **66**, 113101 (2002).
[4] Y.-Y. Chen and Z. Ye, Phys. Rev. Lett. **87**, 184301 (2001).
[5] B. Manzanares-Martínez and F. Ramos-Mendieta, Phys. Rev. B **68**, 134303 (2003).
[6] *Waves and Imaging Through Complex Medias*, edited by P. Sebbah (Kluwer, Dordrecht, 2001), and references therein.
[7] P. Sheng, *Introduction to Wave Scattering, Localization, and Mescoscopic Phenomena* (Academic Press, New York, 1995).
[8] C. Tian and A. Larkin, Phys. Rev. Lett. **95**, 246601 (2005), and references therein.
[9] A. Ishimaru, *Wave Propagation and Scattering in Random Media* (Oxford University Press, New York, 1997).
[10] See, for example, A. Khelif, B. Djafari-Rouhani, J. O. Vasseur, and P. A. Deymier, Phys. Rev. B **68**, 024302 (2003), and references therein.
[11] E. Centeno and D. Cassagne, Opt. Lett. **30**, 2278 (2005), and references therein.
[12] S. G. Johnson, P. Bienstman, M. A. Skorobogatiy, M. Ibanescu, E. Lidorikis, and J. D. Joannopoulos, Phys. Rev. E **66**, 066608 (2002).
[13] V. Lousse and S. Fan, Phys. Rev. B **72**, 075119 (2005).
[14] A. M. Freyria, E. Chignier, J. Guidollet, and P. Louisot, Biomaterials **12**, 111 (1991).
[15] H. Karacali, S. M. Risser, and K. F. Ferris, Phys. Rev. E **56**, 4286 (1997).
[16] E. Conwell, Appl. Phys. Lett. **23**, 328 (1973); **25**, 40 (1974).
[17] Z. Ye, Appl. Phys. Lett. **65**, 3173 (1994); J. Appl. Phys. **78**, 6389 (1995).
[18] S. Kuchinsky, V. Golyatin, and A. Kutikov, Proc. SPIE **5000**, 59

(2003); B. Momeni and A. Adibi, Appl. Phys. Lett. **87**, 171104 (2005).
[19] L. Dong, G. Q. Gu, and K. W. Yu, Phys. Rev. B **67**, 224205 (2003), and references therein.
[20] J. P. Huang, K. W. Yu, G. Q. Gu, and M. Karttunen, Phys. Rev. E **67**, 051405 (2003).
[21] J. J. Xiao, K. Yakubo, and K. W. Yu, Phys. Rev. B **73**, 054201 (2006).
[22] A. A. Maradudin, E. W. Montroll, and G. H. Weiss, *Theory of Lattice Dynamics in the Harmonic Approximation*, Solid State Physics, Suppl. 3 (Academic, New York, 1963), p. 56.
[23] *Ill-Condensed Matter*, edited by R. Balian, R. Maynard, and G. Toulous (North-Holland, Amsterdam, 1979).
[24] F. Wegner, Z. Phys. B **36**, 209 (1980).
[25] T. Nakayama, M. Takano, K. Yakubo, and T. Yamanaka, Opt. Lett. **17**, 326 (1992).
[26] H. Noro and T. Nakayama, J. Opt. Soc. Am. A **14**, 1451 (1997).
[27] Z. S. Popovic and S. Satpathy, Phys. Rev. Lett. **94**, 176805 (2005).
[28] P. J. Michalski, N. Sai, and E. J. Mele, Phys. Rev. Lett. **95**, 116803 (2005).
[29] J. Chadwick, J. Phys. A **32**, 4087 (1999).
[30] B. Cowan, *Nuclear Magnetic Resonance and Relaxation* (Cambridge University Press, New York, 1997).
[31] P. Tong, B. Li, and B. Hu, Phys. Rev. B **59**, 8639 (1999).
[32] A. Dhar, Phys. Rev. Lett. **86**, 5882 (2001).
[33] A. Dhar and B. S. Shastry, Phys. Rev. B **67**, 195405 (2003); L. W. Lee and A. Dhar, Phys. Rev. Lett. **95**, 094302 (2005).
[34] G. A. Narvaez, J. Kim, and J. W. Wilkins, Phys. Rev. B **72**, 155411 (2005).
[35] D. Bria and B. Djafari-Rouhani, Phys. Rev. E **66**, 056609 (2002).